The tail-anchoring domain of Bfl1 and HCCS1 targets mitochondrial membrane permeability to induce apoptosis

Jae-Kyun Ko[1], Kyoung-Han Choi[1], Zui Pan[1], Peihui Lin[1], Noah Weisleder[1], Chul-Woo Kim[2] and Jianjie Ma[1,*]

[1]Department of Physiology and Biophysics, Robert Wood Johnson Medical School, 675 Hoes Lane, Piscataway, NJ 08854, USA
[2]Department of Pathology, Tumor Immunity Medical Research Center and Cancer Research Institute, Seoul National University College of Medicine, Seoul, Korea
*Author for correspondence (e-mail: maj2@umdnj.edu)

Accepted 13 June 2007
Journal of Cell Science 120, 2912-2923 Published by The Company of Biologists 2007
doi:10.1242/jcs.006197

Summary

Many Bcl2 family proteins target intracellular membranes by their C-terminal tail-anchor domain. Bfl1 is a bi-functional Bcl2 family protein with both anti- and pro-apoptotic activities and contains an amphipathic tail-anchoring peptide (ATAP; residues 147-175) with unique properties. Here we show that ATAP targets specifically to mitochondria, and induces caspase-dependent apoptosis that does not require Bax or Bak. Mutagenesis studies revealed that lysine residues flanking the ATAP sequence are involved in targeting of the peptide to the mitochondrial membrane, and charged residues that contribute to the amphipathic nature of ATAP are critical for its pro-apoptotic function. The ATAP sequence is present in another tumor suppressor gene, *HCCS1*, which contains an additional mitochondria-targeting signal (MTS) close to the ATAP. We propose that both ATAP and MTS could be used as therapeutic peptides to induce cell death in the treatment of cancer cells.

Supplementary material available online at
http://jcs.biologists.org/cgi/content/full/120/16/2912/DC1

Key words: ATAP, Bfl1, Apoptosis, Tail anchor

Introduction

The biological functions of Bcl2 family proteins are dependent on their subcellular localization, particularly at the mitochondria outer membrane or endoplasmic reticulum. Many Bcl2 family proteins contain a tail-anchor (TA) domain at the C-terminus, which targets their pro- or anti-apoptotic functions to specific intracellular organelles (Borgese et al., 2003; Duriez et al., 2000; Kaufmann et al., 2003). Recent studies have shown that several anti-apoptotic members of Bcl2 proteins contain pro-apoptotic activities that can be revealed through proteolytic cleavage at the N-terminus (Cheng et al., 1997; Clem et al., 1998; Kucharczak et al., 2005). One example is Bfl1, an anti-apoptotic protein that protects cells from various apoptotic stimuli including chemotherapeutic drugs, activation of TNFα receptor, and overexpression of Bax and Bid (Cheng et al., 2000; Duriez et al., 2000; Holmgreen et al., 1999; Wang et al., 1999; Werner et al., 2002; Zhang et al., 2000; Zong et al., 1999). Unlike most other Bcl2 family members, the TA-domain of Bfl1 contains three charged amino acids that are predicted to align on one side of an α-helix within a rich hydrophobic environment, therefore it is named the amphipathic tail-anchoring peptide (ATAP).

The ATAP sequence has been implicated in targeting of Bfl1 to the mitochondrial membrane, because deletion of 17 amino acids at the C-terminus caused mistargeting of Bfl1 from the mitochondria (Ko et al., 2003a). Moreover, Bfl1s, an alternative splice variant of Bfl1 with a different C-terminal sequence, is found to localize to the nucleus (Ko et al., 2003b). Recent studies from our laboratories and others have revealed the bi-functional nature of Bfl1; proteolysis or deletion of the N-terminus of Bfl1 converts this molecule from having an anti-apoptotic function into a pro-apoptotic function (Ko et al., 2003a; Kucharczak et al., 2005; Yang et al., 2005). Thus, it has been suggested that the TA domain of Bfl1 contains pro-apoptotic activity.

In this study, we demonstrate that ATAP is indeed a potent pro-apoptotic molecule that induces mitochondrial permeability transition via its amphipathic property that perturbs the integrity of the mitochondrial membrane. ATAP-mediated apoptosis does not require Bax and Bak, thus it represents a unique peptide-mediated cell death mechanism with potential as a therapeutic agent for treatment of cancer cells. Within the human genome, the ATAP sequence is present in another tumor suppressor gene *HCCS1* (Kim et al., 2002). An additional mitochondria-targeting signal (MTS) at the N-terminus of HCCS1 contributes to its mitochondria targeting and apoptotic function.

Results

The amphipathic tail-anchor domain is conserved in Bfl1 and HCCS1

The gene encoding Bfl1 (*BCL2A1* or BCL2-related protein A1) is located on chromosome 15q24.3 and contains three exons that are transcribed into two alternative splice variants, Bfl1 (175 a.a.) and Bfl1s (163 a.a.) (Ko et al., 2003b). The tail-

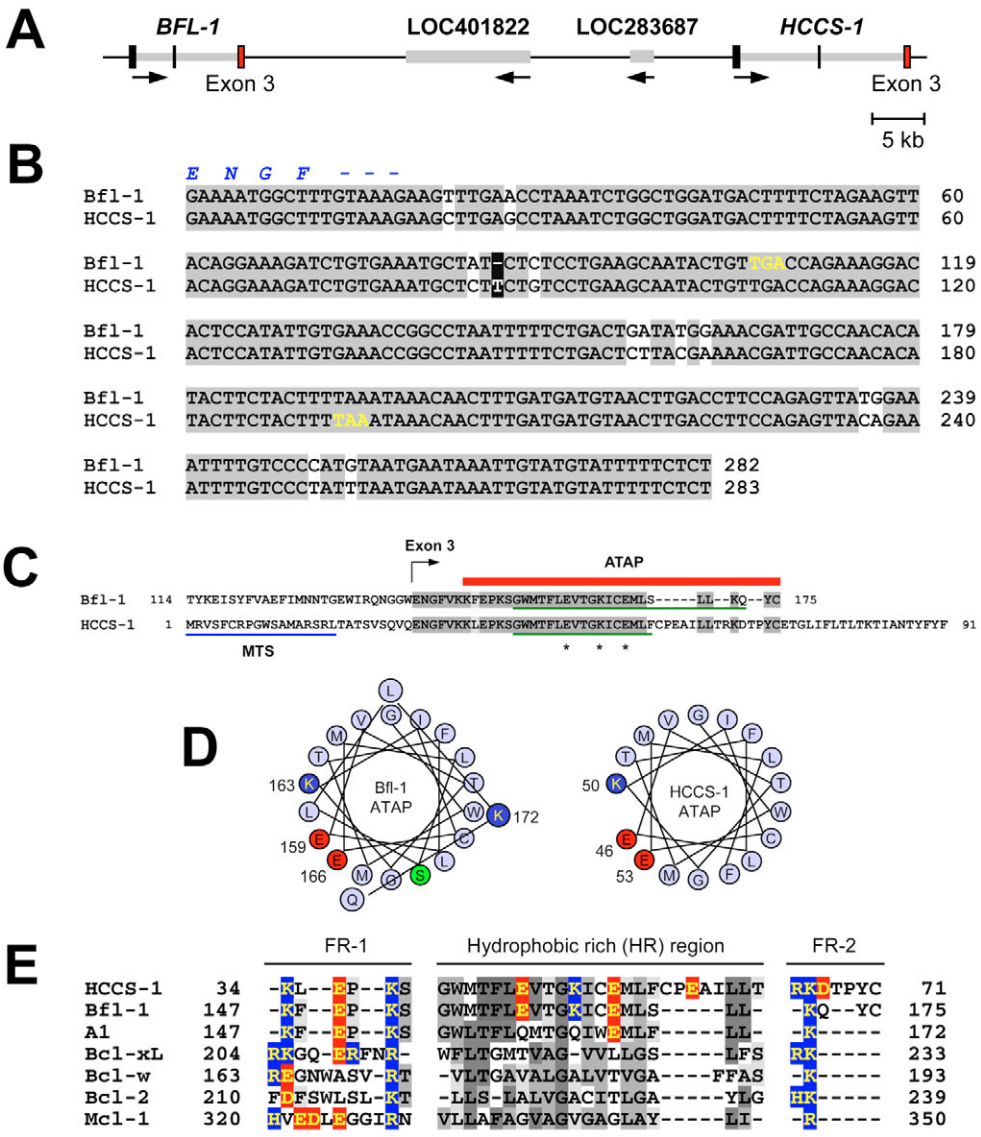

Fig. 1. The amphipathic tail-anchoring peptide (ATAP) is conserved in Bfl1 and HCCS1. (A) Schematic genomic structures of *BCL2A1* (*BFL-1*) and *HCCS1* genes on human chromosome 15q24.3 and 15q25.1, respectively. Black bars indicate exons and red bars indicate conserved exon-3 of *BCL2A1* and *HCCS1* genes. (B) Alignment of exon-3 sequences from *BCL2A1* and *HCCS1* genes. Identical sequences are shaded gray and single base gap is shaded black. Stop codons are yellow. (C) Primary sequence comparison of the TA region of Bfl1 and HCCS1. Horizontal red bar indicates the ATAP sequence of Bfl1 and HCCS1. Green lines indicate predicted α-helical regions. Mitochondrial targeting signal (MTS) of HCCS1 is indicated by a blue line. (D) Helix-wheel diagrams of ATAP sequences of Bfl1 and HCCS1. (E) Amino acid sequence alignment of TA regions from human anti-apoptotic Bcl2 family proteins and A1, a mouse homologue of human Bfl1, and ATAP sequences.

anchoring (TA) domain of Bfl1 (a.a. 147-175) is encoded by exon 3. A database search revealed that exon 3 of *BCL2A1* is conserved in *HCCS1* (16.4 kb) located on 15q25.1 (Fig. 1A). Alignment of the genomic sequences for *BCL2A1* and *HCCS1* showed that an 8.8 kb fragment of *BCL2A1* including exon 3 and the surrounding non-coding regions is highly conserved in *HCCS1*, possibly as a result of duplication of 12 conserved gene segments (see supplementary material Fig. S1).

The genomic sequence of *HCCS1* also contains three exons that encode 91 amino acids (Fig. 1A). The DNA sequence for exon 3 of *HCCS1* is 95% identical to that for *BCL2A1*, and both have identical reading frame starting at E28 for HCCS1 and E141 for Bfl1, respectively (Fig. 1B). HCCS1 contains a 28 amino acid stretch (E28 to L55) that is identical to that of the Bfl1 TA, except for a conservative change at L35 (Fig. 1C). A base-pair deletion in HCCS1 at the 3′ end of exon 3 leads to a frame shift and subsequent changes in the amino acid sequence at the C-terminus of HCCS1.

Sequence alignments showed a common feature with TA domains of all anti-apoptotic members of the Bcl2 protein family, where a hydrophobic-rich segment (HR) was always surrounded by an N-terminal flanking region (FR-1) and a C-terminal flanking region (FR-2) (Fig. 1E). The conserved lysine residues in FR-1 and FR-2 represent potential MTSs for the TA peptide (see below), whereas three charged residues in the HR of Bfl1 (E159, K163 and E166) and HCCS1 (E46, K50 and E53) were unique, since they are not conserved in other Bcl2 family proteins.

Analysis of secondary structures using SOPMA (Geourjon and Deleage, 1995) and Jpred (Cuff et al., 1998) programs predict an α-helical structure for the TA peptide (Fig. 1C). Alignment of amino acids in a α-helical wheel plot revealed the amphipathic nature of the TA peptide from both Bfl1 and HCCS1, with the three charged residues aligning on one side of the α-helix (Fig. 1D). Therefore, we named this domain the amphipathic tail-anchoring peptide (ATAP).

ATAP induces apoptosis independent of Bax and Bak.

To test the cellular function of ATAP, a Flag-ATAP fusion peptide was transiently expressed in HEK293 cells to allow for

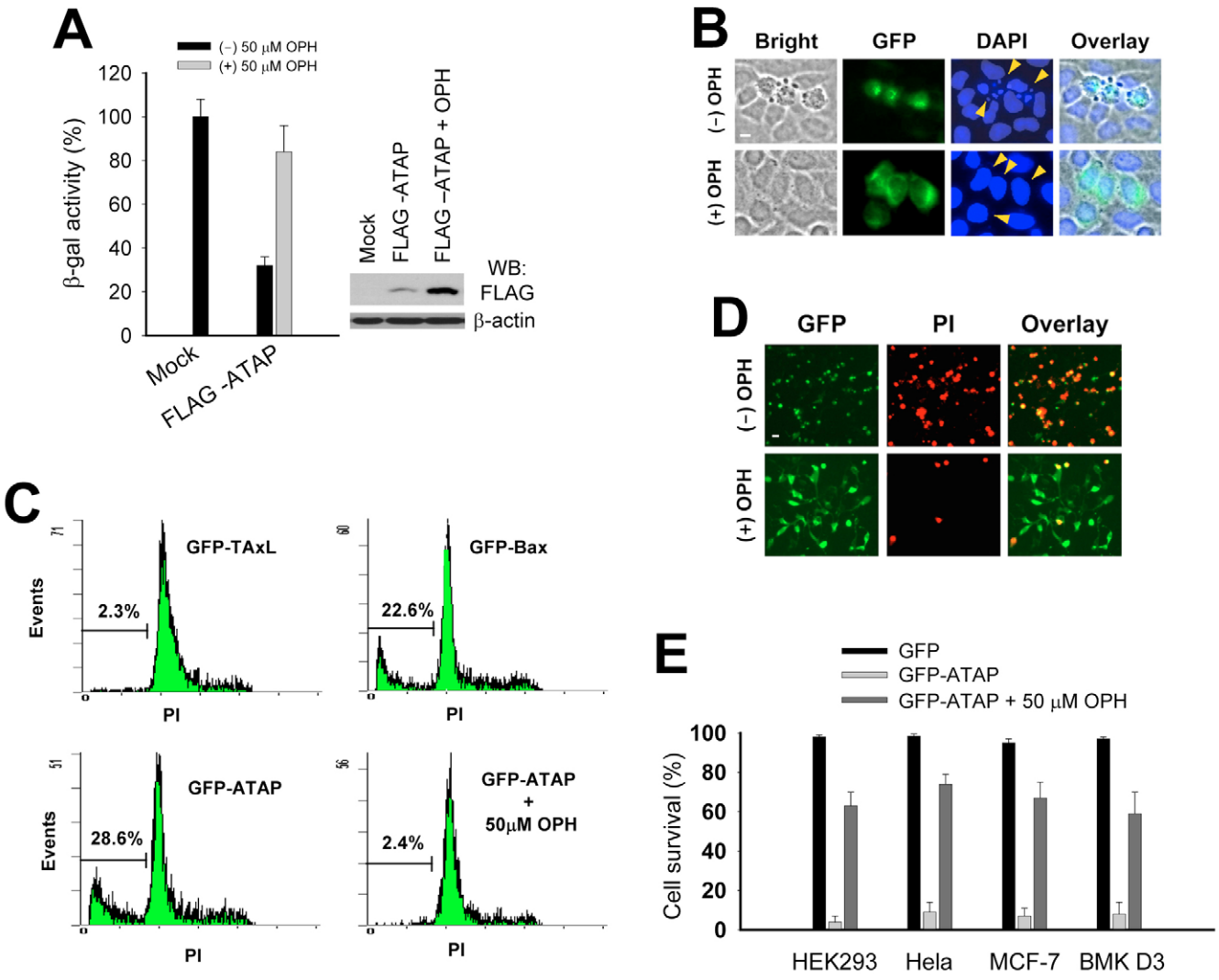

Fig. 2. ATAP-induced apoptosis is independent of Bax and Bak activities. (A) Transient expression of Flag-ATAP induced caspase-dependent cell death of HEK293 cells. Cells were co-transfected with 1 μg of mock or Flag-ATAP expression plasmid with 0.1 μg pCMV-β-gal in the absence or presence of 50 μM OPH. Cell viability was measured by β-galactosidase activity relative to control cells transfected with mock plasmid and the pCMV-β-gal reporter plasmid (left). The relative expression levels of the Flag-ATAP peptide was determined by western blotting with an antibody against the Flag tag epitope (right). (B,C) Transient expression of GFP-ATAP-induced apoptotic nucleus morphology and sub-G1 population in a caspase-dependent manner. GFP-ATAP-transfected HeLa cells were fixed, stained with DAPI and observed under fluorescence microscope 24 hours after transfection (B). HEK293 cells were transiently transfected with the indicated expression plasmids. 18 hours after transfection, cells were harvested, fixed, and stained with PI. The DNA content of GFP-positive cells was then analyzed by flow cytometry (C). (D) Transient expression of GFP-ATAP induced acute cell death in a variety of cancer cells, including HEK293, HeLa, caspase-3 deficient MCF-7 cells and BMK D3 cells derived from the kidney of neonatal knockout mice for Bax and Bak genes. 24 hours after transfection, cell survival was measured by PI exclusion. Representative images taken from HEK293 cells are shown. (E) The percentage of surviving cells was determined by the ratio of PI-negative cells to total GFP-positive cells. About 300 cells from three different fields were scored. Data are expressed as the mean ± s.e. Bars, 10 μm.

detection of the recombinant protein using anti-Flag antibody (Fig. 2A). Twenty-four hours after transfection, the cytotoxic activity of Flag-ATAP was quantified using a β-galactosidase reporter assay (Chittenden et al., 1995; Wood and Newcomb, 2000). With co-transfection of plasmids containing β-galactosidase gene and Flag-ATAP cDNA, the decrease in β-galactosidase activity reflects the loss of cell viability. Compared with cells co-transfected with the mock plasmid, a 68.1±3.9% (n=5) decrease in β-galactosidase activity was observed in cells transfected with Flag-ATAP, which could be prevented by the addition of 50 μM OPH, a pan-caspase inhibitor (Fig. 2A). Moreover, elevated expression of Flag-ATAP was observed in cells treated with OPH, suggesting that either ATAP is a potent trigger of cell death or the peptide is targeted for proteolytic degradation in cells undergoing apoptosis.

We assembled a GFP-ATAP fusion construct to allow live-cell imaging of ATAP-induced cell death. As shown in Fig. 2B, cells transiently expressing GFP-ATAP displayed a condensed and fragmented chromatin structure, illustrating

the apoptotic nature of cell death. The GFP-ATAP-induced chromatin fragmentation could be prevented with the addition of OPH. Quantitative analysis of GFP-ATAP-induced apoptosis in HEK293 cells was performed using FACS assays, where elevation of the sub-G1 cell population was used as an index for cells undergoing apoptosis (Fig. 2C). Clearly, the pro-apoptotic activity of GFP-ATAP is similar to, or perhaps stronger than, that of GFP-Bax, a well-known pro-apoptotic protein (Pan et al., 2001; Smaili et al., 2001) (Fig. 2C). As a control, we found that expression of GFP-TAxL, containing the Bcl-xL TA domain (a.a. 202-233) attached to the C-terminus of GFP, did not show any toxic activity in HEK293 cells.

To test whether there were any cell-type dependent effects of ATAP, GFP-ATAP was transiently expressed in cell lines with different genetic backgrounds. In addition to HEK293 and HeLa cells, we tested GFP-ATAP in MCF-7, a caspase-3 deficient human breast cancer cell line (Janicke et al., 1998), and BMK-D3, a baby mouse kidney cell line derived from *bax*$^{-/-}$*bak*$^{-/-}$ mice (Degenhardt et al., 2002). Cell death analyses using the propidium iodide (PI) exclusion method revealed that >90% of all cell types underwent apoptosis after transient expression of GFP-ATAP (Fig. 2D,E). Since pronounced apoptosis is observed in BMK-D3 cells that lack Bax and Bak (Fig. 2E and supplementary material Fig. S2), the pro-apoptotic activity of GFP-ATAP does not require the participation of Bax and Bak. Moreover, the strong pro-apoptotic effect of GFP-ATAP on MCF-7 cells suggests that ATAP can act through caspases other than caspase-3.

The amphipathic nature of ATAP is essential for its pro-apoptotic activity

Since the charged residues in the HR of Bfl1 and HCCS1 are not present in other Bcl2 family proteins, and since they contribute to the amphipathic nature of ATAP, we tested the contribution of E159, K163 and E166 to the pro-apoptotic function of ATAP in Bfl1 through site-directed mutagenesis. To allow the determination of subcellular localization, the various ATAP mutants were fused with GFP (Fig. 3A). While mutation of a single residue has little effect on the apoptotic activity of ATAP, double mutations, e.g. E159Q-E166Q (mHR3) or E159L-E166L (mHR4), markedly reduce the pro-apoptotic function of ATAP (Fig. 3B). An additional mutation (K163L) in mHR3 further decreased toxicity of ATAP in mHR7. Interestingly, the mHR5 construct containing the E159K-E166K mutation did not appear to affect the pro-apoptotic activity of ATAP (Fig. 3B), suggesting that conservation of charge rather than the polarity of the charge is involved in its pro-apoptotic function. Using the β-galactosidase reporter assay, we found that Flag-mHR3, in which the GFP sequence is replaced with the Flag sequence, also displayed significantly reduced cytotoxic effect compared with the Flag-ATAP construct. Twenty-four hours after transfection, β-galactosidase activity was 26.0±5.2% in Flag-ATAP-transfected cells, whereas it was 62.0±7.8% in Flag-mHR3-transfected cells (n=5, P<0.001) (Fig. 3C), compared with enzyme activity from GFP-transfected cells.

To test whether the amphipathic nature of ATAP is also involved in the apoptotic function of HCCS1, corresponding mutations of charged residues were introduced into the full-length *HCCS1* gene. As shown in Fig. 3D, HCCS1-GFP (E46Q/E53Q) containing mutations corresponding to mHR3 of the Bfl1 ATAP exhibited significantly reduced cytotoxic activity. In further studies, we also tested the effect of ATAP and mHR7 in BMK-D3 cells lacking the expression of Bak and Bax, and in CHO cells stably transfected with Bcl-xL (Pan et al., 2000) (see supplementary material Fig. S2). A similar cytotoxic effect of ATAP was observed in parental CHO cells compared with CHO cells overexpressing Bcl-xL, and in BMK-wt cells compared with BMK-D3 cells, suggesting that the pro-apoptotic function of ATAP is independent of Bax, Bak and Bcl-xL. Moreover, although GFP-ATAP showed potent cytotoxic effects on both CHO and BMK cell lines, GFP-mHR7 showed little cytotoxicity. Taken together, these results demonstrate that the pro-apoptotic activity of ATAP is closely related to the amphipathic property of the peptide.

ATAP targets mitochondria permeability transition to induce apoptosis

Confocal microscopic imaging showed that mutations at E159, E166 or K163 of ATAP did not alter its intracellular targeting properties. Indeed, all mHR1 to mHR7 mutants are localized to the mitochondrial membrane, similarly to the wild-type GFP-ATAP, based on co-localization pattern with mRFP-Mito transiently expressed in HeLa cells (Fig. 4C). Previous studies from other investigators have shown that positively charged residues located at the N-terminus or C-terminus of the TA domain are involved in targeting of the TA peptide to mitochondria (Borgese et al., 2003; Kaufmann et al., 2003). We found that the conserved lysine residues located in FR-1 and FR-2 played a critical role in targeting of ATAP to the mitochondria membrane (Fig. 4). Although mutation of single lysine residues, K147L, K151L or K172L, did not appear to alter the mitochondrial-targeting property of ATAP, double mutation of K147L-K151L (mFR4) caused mistargeting of GFP-ATAP away from the mitochondria (Fig. 4C). The mFR4 mutant localized mainly to the cytoplasm and often formed cytosolic or perinuclear aggregates, with remarkably reduced pro-apoptotic activity compared with the other mFR constructs (Fig. 4B).

In cells undergoing apoptosis, the degradation of chromosomal DNA can be measured in the sub-G1 population of cells containing lower DNA content than healthy cells, or can be detected as a DNA ladder of about 180 bp on an agarose gel. As shown in Fig. 4D, HEK293 cells expressing GFP-ATAP and mHR5 displayed a significantly higher percentage of sub-G1 cells with a more extensive DNA laddering pattern than those expressing mFR4, mHR3, mHR4 or mHR7, confirming the apoptotic nature of cell death induced by ATAP. The time-dependent effects of the various ATAP mutants on apoptosis were further assayed using the PI exclusion method (Fig. 4E). Forty-eight hours after transfection of HEK293 cells with either ATAP or mHR5, more than 95% of cells were PI positive, whereas only about 38% of cells were PI positive with expression of either mHR3 or mHR4. In the case of mHR7-transfected cells, only 19% cells were PI positive at the 48-hour time point (Fig. 4E). Interestingly, cells transfected with mFR4 exhibited progressive cell death at later stages of the experiment (e.g. more than 36 hours after transfection). Although the mitochondrial targeting of mFR4 seemed to be impaired, a portion of the protein was detected at the mitochondria (Fig. 4C). One possibility is that the delayed

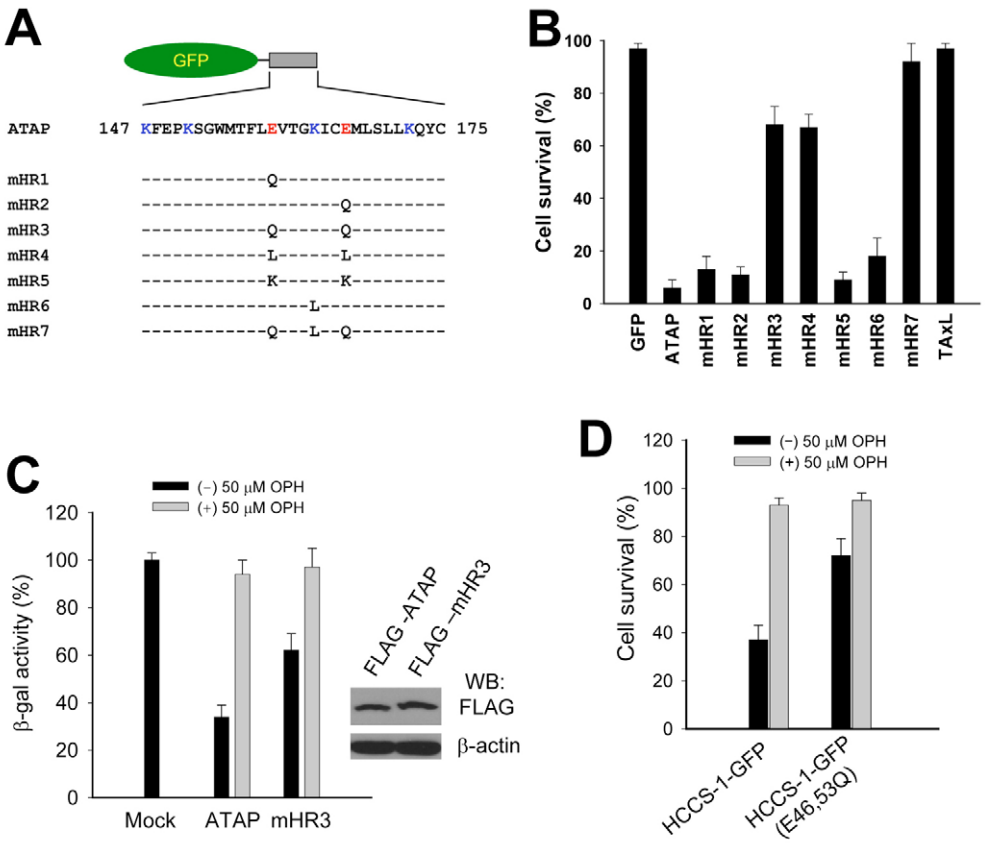

Fig. 3. The pro-apoptotic activity of ATAP requires an amphipathic property. (A) Schematic representation of the GFP-ATAP constructs in which point mutations were introduced into the hydrophobic rich (HR) region of the ATAP. (B) Cell survival was measured by PI exclusion in the HEK293 cells transfected with 1 μg GFP-ATAP mutant constructs 24 hours after transfection. (C) Flag-mHR3 peptide showed reduced pro-apoptotic activity. HEK293 cells were co-transfected with 0.1 μg pCMV-β-gal reporter plasmid and 1 μg of the Flag-ATAP or Flag-mHR3 expression plasmids. 24 hours after co-transfection, cell viability was measured by β-galactosidase activity (left). The relative expression levels of the Flag-tagged peptides were determined by western blotting with an antibody against the Flag tag epitope (right). (D) Involvement of amphipathic nature of ATAP in the apoptotic function of HCCS1. HEK293 cells were co-transfected with 0.1 μg pCMV-β-gal reporter plasmid and 1.0 μg HCCS1-GFP or HCCS1-GFP (E46Q/E53Q) containing mutations corresponding to mHR3 of the Bfl1 ATAP. 24 hours after co-transfection, cell viability was measured by β-galactosidase activity. Data are expressed as the mean ± s.e.

toxic effect of mFR4 results from the gradual accumulation of the molecule at the mitochondrial membrane.

One particular exception is found with the mFR7 mutant, where all three lysine residues in FR-1 and FR-2 were mutated to leucines. Unlike mFR4, mFR7 still maintained its targeting to mitochondria and possessed a potent pro-apoptotic activity (Fig. 4B). Analysis of the primary amino acid sequence of GFP-mFR7 identified other charged residues from the C-terminal portion of GFP and the multiple cloning site (MCS) of the pEGFP-C1 plasmid that resides proximal to the ATAP sequence. This external sequence resembles the FR-1 region of Bcl-xL in terms of charge contents and positioning, which could act as surrogate for the MTS in the absence of positively charged residues within the Bfl1 flanking regions (see supplementary material Fig. S3). Indeed, deletion of these positively charged residues eliminated the mitochondrial targeting of mFR7 and consequently its pro-apoptotic function. Moreover, insertion of an 11 amino acid linker sequence into the MCS also eliminated mitochondrial targeting of mFR7 and reduced its apoptotic activity. These results are consistent with previous studies of Kaufmann et al. (Kaufmann et al., 2003) and further suggest that charged residues must remain adjacent to HR segment for efficient targeting of ATAP to MOM.

Overall, our data suggest that lysine residues located in the N-terminal flanking regions of ATAP are essential for targeting of ATAP to mitochondria, and that the pro-apoptotic activity of ATAP is closely linked to its association with mitochondria.

Both the MTS and ATAP are involved apoptosis induced by HCCS1

The primary amino acid structure of HCCS1 contains a stretch of 18 amino acids (a.a. 1-18) that are proximal to the ATAP sequence, and may act as an alternative MTS for HCCS1 (see Fig. 1C). To explore the contribution of MTS and ATAP to the apoptotic function of HCCS1, we generated GFP fusion constructs with various HCCS1 deletion mutants (Fig. 5A). Due to the high level of toxicity produced by ATAP, it was necessary to include 50 μM OPH in the cell culture medium in experiments where we visualize the mitochondrial localization patterns of the various GFP fusion constructs.

As shown in Fig. 5B, HCCS1-GFP, as well as GFP-ATAP (HCCS1), exhibited close co-localization with mRFP-Mito in

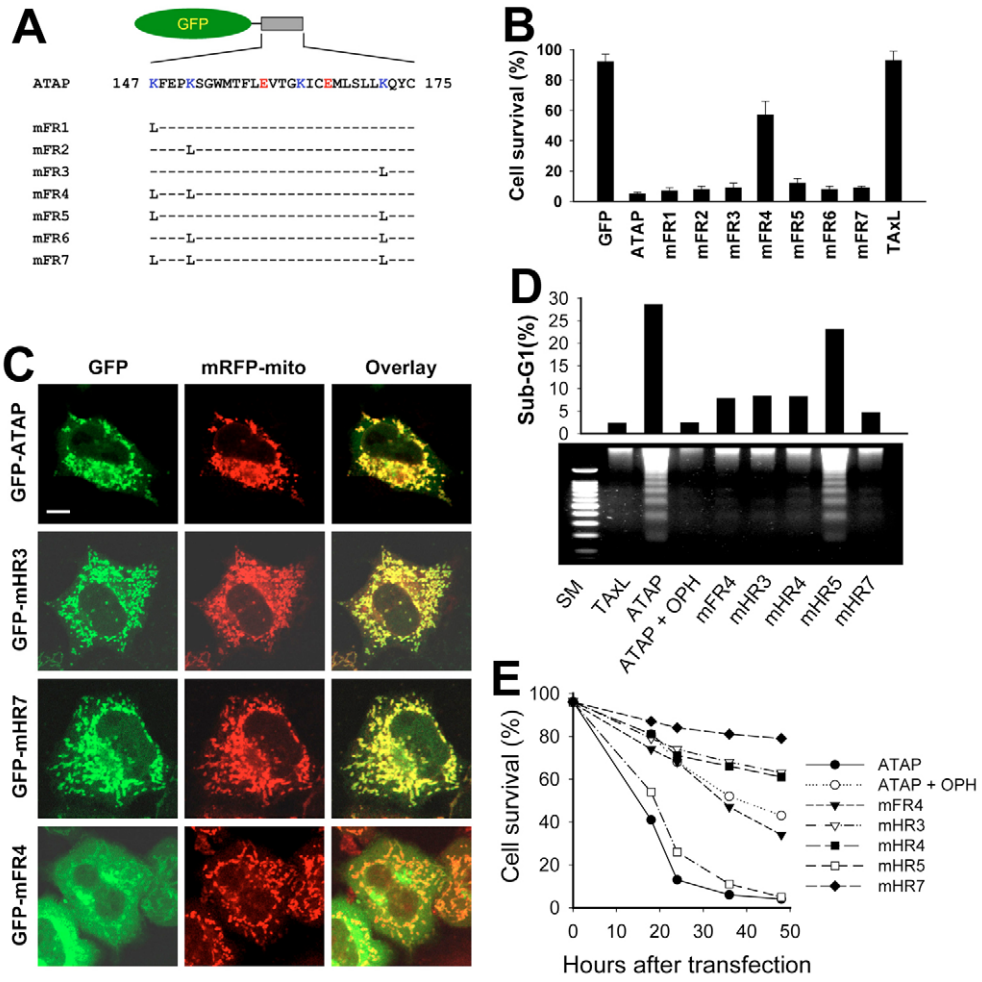

Fig. 4. The pro-apoptotic activity of ATAP involves targeting to mitochondria. (A) Schematic representation of the GFP-ATAP constructs in which point mutations were introduced into the flanking regions of the ATAP. (B) Cell survival was measured by PI exclusion in the HEK293 cells transfected with 1 μg GFP-ATAP mutant constructs 24 hours after transfection. (C) Subcellular localization of ATAP mutants fused with GFP. HeLa cells were transfected with 0.5 μg of the indicated plasmids. Cell culture was performed in the presence of 50 μM OPH to prevent rapid cell death. 18 hours after transfection, cells were incubated in medium containing 50 nM MitoTracker for 2 hours and fixed using 4% paraformaldehyde. Localization of GFP fusion proteins was observed using confocal microscopy. Bar, 10 μm. (D) Cellular effects of GFP-ATAP mutants on apoptosis. HEK293 cells were transiently transfected with the indicated plasmids expressing ATAP mutants fused with GFP. 18 hours after transfection, cells were harvested, fixed, and stained with PI. The DNA content of GFP-positive cells was then analyzed by flow cytometry (upper panel). DNA fragmentation was also analyzed by electrophoresis on 2% agarose gels (lower panel). SM, 100 bp ladder size marker. (E) Time-course effect of GFP-ATAP and GFP-ATAP mutants on HEK293 cells. Cell survival was measured by PI exclusion in the HEK293 cells transfected with 1 μg GFP-ATAP mutant constructs.

HeLa cells, demonstrating the specific targeting of HCCS1 at the mitochondria membrane. Attachment of GFP to the N-terminus of HCCS1 lacking MTS, GFP-HCCS1 (ΔMTS), also revealed a characteristic mitochondria localization pattern, confirming our observation that the ATAP domain of HCCS1 contained an intrinsic MTS. Interestingly, attachment of GFP to the C-terminus of HCCS1 lacking MTS caused mistargeting of HCCS1 (ΔMTS)-GFP away from the mitochondria. This is consistent with earlier studies demonstrating that addition of a large moiety to the C-terminal end of TA proteins disrupted their intracellular targeting properties (Johnston et al., 2002).

The MTS-GFP also exhibited a typical mitochondrial localization pattern, indicating that the MTS domain of HCCS1 possesses mitochondrial-targeting properties (Fig. 5B). Therefore, HCCS1 contains dual targeting signals for mitochondrial localization, one at the N-terminus (MTS) and one at the C-terminus (ATAP). Cell viability analyses using the PI exclusion method showed that MTS-GFP had no toxic effect in HeLa cells, whereas HCCS1-GFP, GFP-HCCS1 (ΔMTS) and GFP-ATAP (HCCS1) all exhibited potent pro-apoptotic activities that could be inhibited by OPH. Moreover, HCCS1 (ΔMTS)-GFP, which mistargets from mitochondria, displayed significantly lower cytotoxicity (Fig. 3C). These results further support the notion that ATAP is responsible for the pro-apoptotic activity of HCCS1 and that mitochondrial targeting is required for the pro-apoptotic function of HCCS1.

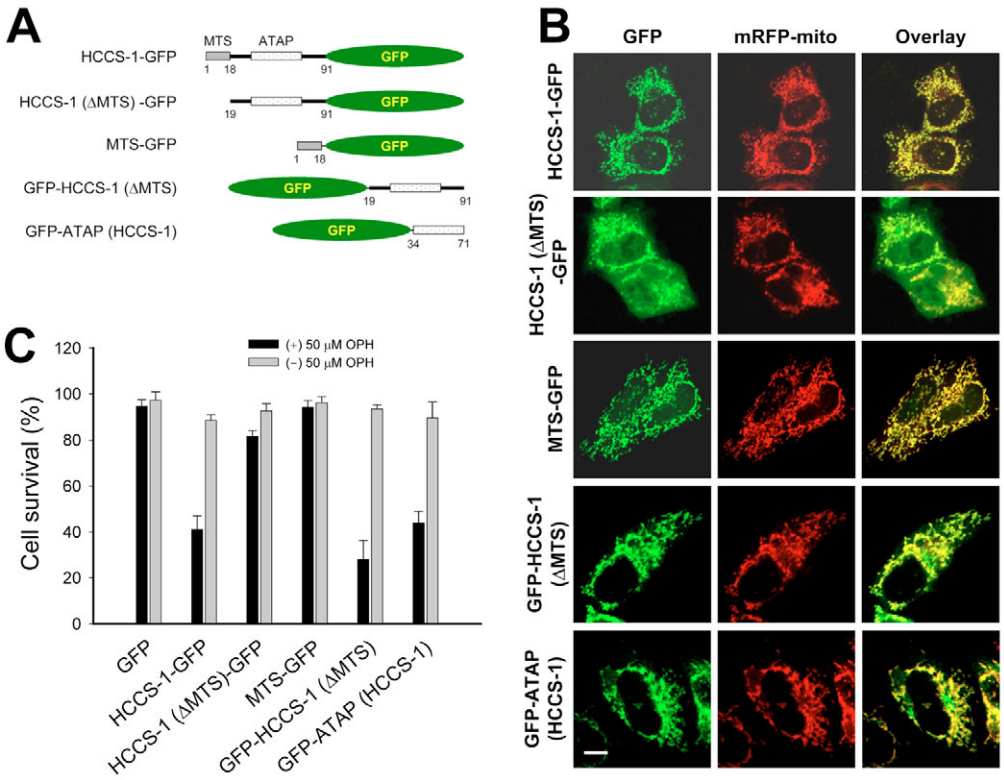

Fig. 5. Both MTS and ATAP are involved in mitochondrial-targeting apoptosis induced by HCCS1. (A) Schematic representation of the GFP fusion proteins of HCCS1 and its deletion mutants. (B) Subcellular localization of GFP fusion proteins. HeLa cells were transfected with 0.5 μg of the indicated plasmids. Cell culture was performed in the presence of 50 μM OPH. 18 hours after transfection, cells were incubated in medium containing 50 nM MitoTracker for 2 hours and fixed using 4% paraformaldehyde. Localization of GFP fusion proteins was observed using confocal microscopy. Bar, 10 μm. (C) Cell survival was measured by PI exclusion in the HEK293 cells transfected with 1 μg GFP fusion constructs 24 hours after transfection.

ATAP perturbs membrane permeability in lipid bilayer assay

Extensive studies have shown that loss of mitochondrial membrane potential acts as a trigger for cytochrome c release and caspase activation in apoptosis signaling (Petit et al., 1995; Zamzami et al., 1995). To determine whether the loss of mitochondrial membrane potential is directly involved in ATAP-induced apoptosis, we monitored mitochondrial membrane potential in HeLa cells using MitoTracker Red (CM-H_2 TMRos), which targets mitochondria and develops fluorescence by oxidation, only in cells with intact mitochondrial membrane potential. HeLa cells were transfected with GFP-ATAP, GFP-mHR7 or GFP-TAxL, in the presence of 50 μM OPH to reduce the downstream effect of caspase activation on mitochondrial integrity. Although most of cells transfected with GFP-TAxL were healthy with bright MitoTracker staining, a majority of the GFP-ATAP transfected cells showed diffuse and low intensity MitoTracker staining (Fig. 6A). On average, 65.0±8.7% (n=5) of HeLa cells expressing GFP-ATAP were MitoTracker negative, whereas only 19.0±9.3% of those expressing GFP-TAxL were MitoTracker negative (Fig. 6B). However, cells transfected with GFP-mHR7 showed increased MitoTracker staining that was comparable that in cells transfected with GFP-TAxL. Similar results were obtained with the other mHR and mFR mutant constructs, where development of MitoTracker labeling is closely associated with the reduced toxic effects of the ATAP constructs (not shown). These results indicate that ATAP-induced apoptosis could involve the direct induction of mitochondria outer membrane permeabilization.

Cytochrome c release is a critical step in the initiation of the mitochondrial apoptosis pathway. To test the effect of ATAP and mHR7 on cytochrome c release from mitochondria, we performed two complementary assays. First, using transient expression of GFP-ATAP in HEK293 cells, we found that a significant portion of cytochrome c is released into the cytosol in cells transfected with GFP-ATAP, whereas GFP-mHR7 does not produce significant cytochrome c release (Fig. 6C, left). Second, using isolated mitochondria membrane preparations from BMK-D3 cells, we found that addition of synthetic ATAP peptide induced release of cytochrome c – an effect that was not observed with mHR7 peptide (Fig. 6C, right).

As a direct test of the effects of ATAP on the integrity of cellular membranes, we performed electrophysiological studies using the lipid bilayer reconstitution system (Lam et al., 1998; Ma et al., 1988). The toxic effect of ATAP in *E. coli* (not shown) prevents purification of the peptide in sufficient quantity for our functional studies. Therefore, synthetic ATAP peptides were used in our bilayer reconstitution assays. As shown in Fig. 6D, addition of the wild-type ATAP peptide (11

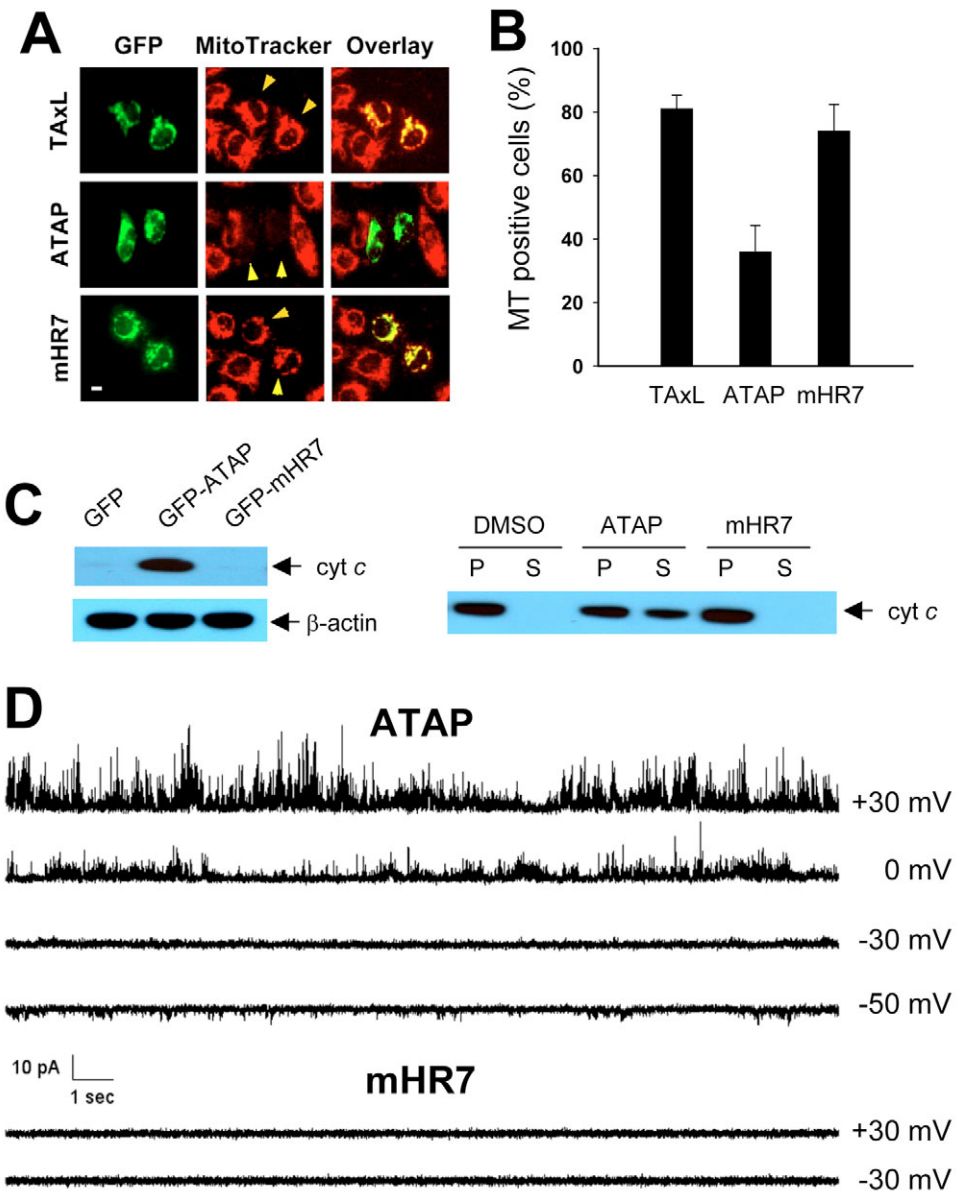

Fig. 6. ATAP induces the loss of mitochondrial membrane potential and perturbs membrane permeability in planar lipid bilayers. (A) Effect of GFP-ATAP on the mitochondrial membrane potential. Mitochondrial outer membrane potential was observed using MitoTracker Red (CM-H_2 TMRos) dye. HeLa cells were transfected with GFP-ATAP, GFP-mHR7 or GFP-TAxL and cultured in the presence of 50 μM OPH. 24 hours after transfection, cells were incubated in medium containing 50 nM of MitoTracker for 2 hours and observed under a fluorescence microscope. Bar, 10 μm. (B) Green (GFP) and red (MitoTracker) double-positive cells were quantified from about 300 GFP-positive cells from three different fields. Data are expressed as the mean ± s.e. (C) Effect of ATAP on cytochrome c release. Left panel, HEK293 cells were transfected with 1 μg of pEGFP (lane 1), pEGFP-ATAP (lane 2) or pEGFP-mHR7 (lane 3). 20 μg mitochondria-free cytosol proteins were analyzed by western blotting using anti-cytochrome c antibody. Right panel, mitochondria membrane isolated from BMK-D3 cells were incubated with synthetic ATAP and mHR7 peptides (100 μM). ATAP induced cytochrome c release into the supernatant (S), whereas cytochrome c remained in the pellet (P) in preparations treated with mHR7 and DMSO (as a control). (D) Effect of synthetic ATAP and mHR7 peptides on the membrane permeability of planar lipid bilayer. The peptides (11.1 μM) were added to the *cis* chamber. Current traces at the corresponding holding potentials were measured from recording solution of 200 mM KCl (*cis*) and 50 mM NaCl (*trans*). Data are representative of n=5 for ATAP and n>35 for mHR7.

μM) produced a significant effect on the permeability of the lipid bilayer membrane to monovalent cations. In a recording solution containing 200 mM KCl (*cis*) and 50 mM NaCl (*trans*), outward current from *cis* to *trans* was measured at 0 mV holding potential, suggesting that ATAP influences the cation permeability of the lipid bilayer membrane (n=5). Although the current traces fluctuate at variable levels without a definable unitary conductance, a clear reversal potential for currents was measured at ~–30 mV, which is close to the Nernst potential for cations. ATAP at higher concentrations (>22.2 μM) often caused instability of the bilayer membrane, with rupture of the lipid bilayer occurring within 30 minutes of addition of the peptide (n>30). Thus, high concentrations of ATAP could affect the permeability of the lipid bilayer membrane, without forming a stable pore structure. In parallel experiments, we found that the mHR7 mutant peptide did not induce any notable changes in membrane conductance, at concentrations of 11-44 μM (n=35, Fig. 6D). This result is consistent with the reduced apoptotic activity of the mHR7 protein transiently expressed in cells.

Discussion

Previous studies have demonstrated a bifunctional property of Bfl1, with the full-length protein containing the recognized anti-apoptotic activity and the N-terminus deletion mutants displaying potent pro-apoptotic activities (Ko et al., 2003a; Yang et al., 2005). A recent study by Kucharczak et al. (Kucharczak et al., 2005) showed that TNFα receptor activation results in in-vivo proteolysis of Bfl1 by the proteosome and calpain-like protease, thus converting Bfl1 into a pro-apoptotic molecule. As a result, it has been hypothesized that Bfl1 contains an intrinsic pro-apoptotic function that is normally inhibited by anti-apoptotic moieties to account for the anti-apoptotic nature of the full-length Bfl1 protein. Here we demonstrate that the ATAP of Bfl1 and HCCS1 displays potent pro-apoptotic activities that result from two conserved

functional motifs, one that allows targeting to mitochondrial membrane and the other that provides an amphipathic property to the peptide.

ATAP targets mitochondria permeability transition to induce apoptosis

We demonstrate that ATAP can induce mitochondria permeability transition and act as a potent stimulator of apoptosis. Although all anti-apoptotic Bcl2 members contain the TA signature motif at their C-termini, ATAPs of Bfl1 and HCCS1 are unique as they contain three charged residues in the middle of the hydrophobic-rich region and therefore are amphipathic in nature. Previously, the ATAP of Bfl1 has been excluded as a bona fide TA on the premise that the existence of charged residues represents a barrier for penetration and partition of the peptide to lipid bilayer membranes (Cory and Adams, 2002; Gross et al., 1999). However, many experimental observations using immunostaining, electron microscopy and subcellular fractionation have shown that Bfl1 targets to the mitochondria of various cell types (Duriez et al., 2000; Werner et al., 2002). Our previous work has shown that deletion of part of the ATAP sequence caused Bfl1 to lose its targeting to the mitochondria (Ko et al., 2003a; Ko et al., 2003b). Here we demonstrate that ATAP is sufficient for localizing a reporter molecule (GFP) at mitochondria. Our results further reveal that three lysine residues within the FR-1 and FR-2 regions are critical for targeting to mitochondria. Interestingly, an external sequence containing basic residues adjacent to the N-terminus of TA could also function as a pseudo-flanking region for mitochondrial targeting in the absence of basic residues within the Bfl1 flanking regions (see supplementary material Fig. S3). This indicates that the position of basic residues at the N-terminus of ATAP is essential for efficient mitochondrial targeting. As a result, potential interference by external charged residues from vector sequence must be considered in future studies for examining the targeting property of TA using fusion constructs with reporter molecules like GFP.

We showed that charged residues located within the HR domain are essential for the pro-apoptotic activity of ATAP. We propose that these charged amino acids (E159, K163 and E166 in Bfl1) are involved in the formation of an aqueous pore to perturb mitochondrial membrane integrity. This seems likely, because we have attempted to purify recombinant ATAP peptide from *E. coli* for our lipid bilayer reconstitution study; however, we could not achieve sufficient quantity of the purified peptide because of the highly toxic effect of ATAP on bacteria (not shown). Using the lipid bilayer reconstitution system, we demonstrated that the synthetic wild-type ATAP peptide produced significant effects to the cation permeability of the lipid bilayer membrane, whereas a mutant mHR7 peptide, which can bind to the mitochondria membrane but is not toxic to the cells, did not affect conductance of the lipid bilayer membrane.

The ATAP-mediated permeability changes in the in vitro system did not display the typical stable conductance behavior one would expect from a pore-forming channel. ATAP could either interact with or modulate the pre-existing channels to alter mitochondrial membrane permeability, or potentially other domains of the Bfl1 or HCCS1 proteins may contribute to changes in membrane permeability observed in vivo. Previously, several MTSs located at the N-terminus of precursor proteins have been shown to induce mitochondrial membrane permeability transition and release of cytochrome c by modulating TOM and TIM translocase complexes (Kushnareva et al., 2001; Muro et al., 2003). Since interaction between Bcl2 and TOM20 has been reported (Schleiff et al., 1997) and localization of Bcl2 is partially dependent on TOM20 (Motz et al., 2002), future studies should focus on investigating whether other mitochondrial proteins such as TOM or TIM complex are involved in the pro-apoptotic function of ATAP.

Pro-apoptotic function of HCCS1 linked to induction of mitochondria permeability transition

In addition to Bfl1, the ATAP sequence appears in HCCS1, a recently identified tumor suppressor gene whose cellular function has yet to be defined (Kim et al., 2002). The genomic sequence of HCCS1 is located in close proximity to that of Bfl1 on chromosome 15. In addition to ATAP, HCCS1 contains a novel MTS at the N-terminus. Since HCCS1 lacking MTS can target to mitochondria and induce caspase-dependent cell death, it suggests that ATAP contributes to the intrinsic mitochondria targeting property for HCCS1. In addition to mitochondria targeting, we also observed parallel changes in the pro-apoptotic activities of ATAP with mutation of the corresponding charged residues in Bfl1 and HCCS1. Our results indicate that the pro-apoptotic function of ATAP is conserved in Bfl1 and HCCS1.

Since the full-length Bfl1 and HCCS1 have opposite functions, one being anti-apoptotic and the other being pro-apoptotic, it is interesting to observe their expression levels in various tissues. Analyses of the available mRNA microarray data and EST expression profiles reveal that the expression of *BCL2A1* and *HCCS1* are mutually exclusive in 16 out of 19 tissues examined (supplementary material Fig. S4), suggesting their possible complementary tissue-specific functions in cell proliferation and regeneration. Interestingly, only the lymph node and kidney were found to contain high level transcripts of both Bfl1 and HCCS1. This result suggests that Bfl1 might share similar biological functions to HCCS1 as a pro-apoptotic factor to achieve dynamic regulation of apoptosis according to cell state at the lymph node and kidney. In support of this hypothesis, Kucharczak et al. (Kucharczak et al., 2005) found that Bfl1 can be converted to pro-apoptotic factor by proteolytic turnover in a FL5.12 pro-B cell line in response to TNFα stimulation, indicating that the pro-apoptotic activity of Bfl1 might be involved during the B-cell selection process that occurs in lymph nodes.

In an attempt to examine the tumor-suppressor function of HCCS1, we used RT-PCR to examine the expression level of *HCCS1* in normal human tissues including lung, breast and cervix, and in various well established cancer cell lines (supplementary material Fig. S4). To discriminate *HCCS1* and *BCL2A1* transcripts, we used primer pairs specific to the exon 1 region of *HCCS1* and *BCL2A1*. In the normal lung, breast and cervix tissues, abundant *HCCS1* products were detected whereas *BCL2A1* products were conspicuously absent, which is consistent with the microarray data, which showed that these tissues contain abundant levels of HCCS1 but not Bfl1. Interestingly, a very low expression level of *HCCS1* was detected in two of six breast cancer cell lines, e.g. MDA-

MB231 and MDA-MB435, indicating a possible role for HCCS1 in tumorigenesis. It is noticeable that HeLa – a cervical cancer cell line – also displayed reduced expression of HCCS1 (supplementary material Fig. S3B). Whether downregulation of HCCS1 is directly involved in the development of cancer cells, and whether altered targeting of HCCS1 plays a role in its pro-apoptotic function, need to be examined further.

ATAP as a potential therapeutic reagent for mitochondria-mediated apoptosis

Two general types of peptides known to trigger mitochondrial apoptosis are currently under clinical trials as potential cancer therapeutic reagents. One type is the amphipathic peptides containing a high content of basic residues derived from anti-bacterial peptides (Chen et al., 2001; Ellerby et al., 1999; Mai et al., 2001). Targeting of these peptides to mitochondria relies on the electrostatic interaction between positively charged residues in the peptides and negatively charged mitochondrial membrane lipids. After targeting to the mitochondrial membrane, these peptides disrupt mitochondrial function and cause cytochrome c release through deformation of lipid membrane or formation of pores at the mitochondrial membrane. This mechanism may be similar to their antimicrobial function on negatively charged bacterial membrane (Shai and Oren, 2001). However, since the cytotoxic activity of these peptides depends on a high intracellular concentration of peptides because of inefficient targeting to mitochondria, their specificity in targeting cancer cells must be maximized to allow effective clinical application. The other class of peptides are those derived from BH3-only pro-apoptotic Bcl2 family proteins such as Bad and Bid (Letai et al., 2002; Schimmer et al., 2001; Walensky et al., 2004). The BH3 peptide of Bid can directly bind to pro-apoptotic Bax and Bak to activate them to induce apoptosis, or can bind to anti-apoptotic Bcl2 and Bcl-xL to prevent their inhibition of Bax and Bak (Letai et al., 2002). A recent study showed that a stabilized BH3 peptide derived from Bid could specifically induce apoptosis of several leukemia cells, highlighting their therapeutic potential (Walensky et al., 2004). However, downregulation of pro-apoptotic protein and/or upregulation of anti-apoptotic protein often provides cancer cells with a resistance mechanism against apoptotic therapeutics. Therefore, an approach where BH3 peptides can overcome this obstacle by providing an effective dose range without side effects on normal cells remains to be determined.

We propose that ATAP could be used as potent reagent for cancer treatment. ATAP is distinguished from the cationic antibacterial peptides by active and specific targeting to the mitochondrial membrane. ATAP is unique from BH3 peptides because of its direct interaction with the mitochondria membrane, which does not require participation of the Bcl2 family proteins. Anti-apoptotic Bcl-xL cannot block ATAP-induced apoptosis and the pro-apoptotic activity of Bax or Bak is not required for the pro-apoptotic function of ATAP. Therefore, ATAP has the potential to overcome the resistance of cancer cells to apoptotic stimuli generated by altered expression levels of Bcl2 family proteins. Here we describe a new strategy for developing cancer therapeutic reagents using the ATAP sequence, which can specifically target mitochondria to disrupt mitochondrial membrane integrity.

Materials and Methods

Plasmid construction

PCR-based mutagenesis and subcloning were used to construct all plasmids used in this study (Ko and Ma, 2005). Primer sequences used for subcloning and mutagenesis are listed in supplementary material Tables S1-S3. PCR product encoding ATAP was amplified using pBfl1-myc (Ko et al., 2003b) as a template, and that encoding the TA of Bcl-xL (E202-K233) was amplified using pEGFP-Bcl-xL plasmid (Ko et al., 2003a) as a template. The PCR products were cloned in-frame behind the GFP sequence into *Xho*I and *Eco*RI sites in pEGFP-C1 (Clontech), to obtain the pGFP-ATAP and pGFP-TAxL plasmids. MGC clone 584619 containing the full-length cDNA of HCCS1 was purchased from ATCC, and used as a PCR template to construct pHCCS1-GFP, pHCCS1 (ΔMTS)-GFP, pMTS-GFP, pGFP-HCCS1 (ΔMTS) and pGFP-ATAP (HCCS1). The plasmids with GFP fused to the 3′ end were generated through subcloning of PCR products into the *Bsp*E1 and *Eco*RI sites of pEGFP-N1 (Clontech) vector. To generate pFLAG-ATAP and pFLAG-mHR3, cDNA fragment encoding GFP of pGFP-TA and pGFP-mHR3 plasmids was replaced by cDNA fragment coding the Flag epitope. We used the following oligos containing 3′ ends of 23 bases complementary (italics) between sense and antisense primers (bold italic). The two overlapping oligos were annealed and subcloned into the *Xho*I and *Eco*RI sites (bold) of pGFP-ATAP and pGFP-mHR3. Flag/FP4-F, 5′-CC**GCTAGC**GCTACCGGTCGCCACCATGGACTACA-AAGACGATGACGACAAGC***TTGAATTCGATTTTCCACCTCCC***-3′; FLAG/FP4-R, 5′-AG**CTCGAG**ATCTGAGTCCGGACTTGTAGCTGCCCAGTTCTTCATCG-GTAGG***GGGAGGTGGAAAATCGAATTCAA***-3′. pHCCS-1-GFP (E46Q/E53Q) was obtained by mutagenesis using *Bsm*BI as described (Ko and Ma, 2005). PCR amplification was performed using pHCCS-1-GFP as a PCR template and the following primers: HCCS-mF, 5′-AA**CGTCTC**AAGGAAAGATCTGTCAGAT-GCTCTTCTGTCCTGAAGCAATA-3′; HCCS-mR, 5′-AA**CGTCTC**ATCCTGTA-ACCTGTAGAAAAGTCATCCAGCCAGATTTA-3′; HCCS-anchor-F, 5′-AA**TC-CGGA**ATGAGAGTTTCATTCTGTCGCCCAGG-3′; HCCS-anchor-R, 5′-AA**G-AATTC**AAAAGTAGAAGTATGTGTTGGCAATCG-3′. The mutant cDNA fragment of HCCS-1 was subcloned into *Bsp*EI and *Eco*RI sites of the pEGFP-N1 vector.

To generate pGFP-linker-ATAP and pGFP-linker-ATAP, mutants including pGFP-linker-mFR7 were generated by substitution of cDNA sequences in pGFP-ATAP and ATAP mutant plasmids with synthetic cDNA fragments encoding GLPAQITFLSVPGSR. The following synthetic oligos were annealed and subcloned into the *Bsp*EI and *Xho*I sites of pGFP-ATAP and ATAP mutant constructs: Linker-F, 5′-**CCGGA**CTCCCCGCCCAGATCACCTTCCTGAGCGT-GCCCGGCT**C**-3′; Linker-R, 5′-**TCGAG**AGCCGGGCACGCTCAGGAAGGTG-ATCTGGGCGGGGAGT-3′.

To construct expression vector mRFP-mito, mRFP (monomeric red fluorescence protein) cDNA fragment was amplified using pRSETB-mRFP (Campbell et al., 2002) as a template. The PCR product was subcloned into *Nhe*I and *Bsp*EI sites of pGFP-TAxL to replace GFP by mRFP and generate pmRFP-mito. All constructs were verified by DNA sequencing.

Bioinformatic analyses

Genomic sequences of human Bfl1 (GeneID 597) and HCCS1 (GeneID 400410) were obtained from GenBank database (http://www.ncbi.nlm.nih.gov/) and homology searches were carried out using the BLAST program (http://www.ncbi.nlm.nih.gov/BLAST). The genomic locations containing *BCL2A1* (Bfl1) and *HCCS1* are NM_004049 on chromosome 15q24.3 region from 78,040 to 78,050 kb, and XM_375224 on chromosome 15q25.1 region from 77,978 to 77,994 kb, respectively. Alignment of the genomic sequences of *BCL2A1* and *HCCS1* was performed with the AVID program using a window size of 100 bp (http://genome.lbl.gov/vista/index.shtml, 23). Alignment of exon sequences and primary amino acid sequences were carried out with the CLUSTALW program (http://www.ebi.ac.uk/clustalw, 24). Secondary structure was predicted using SOPMA (Geourjon and Deleage, 1995) and Jpred (Cuff et al., 1998) programs. The MTS of HCCS1 was inferred using Targetp v1.1 (http://www.cbs.dtu.dk/services/TargetP/, (Emanuelsson et al., 2000; Nielsen et al., 1997).

mRNA expression of Bfl1 and HCCS1 in normal human tissues and cancer cell lines

Initial analysis with distribution of *BCL2A1* and *HCCS1* transcripts in normal human tissues was performed using the available microarray data and EST expression profiles provided by NCBI UniGene server (http://www.ncbi.nlm.nih.gov/UniGene). Semi-quantitative evaluation of *BCL2A1* and *HCCS1* transcripts was analyzed by RT-PCR, using total RNA of human normal lung, breast and cervix were purchased from Stratagene (La Jolla, CA). Total RNA of cancer cell lines was isolated using Tri-reagent (Sigma), according to the manufacturer's instructions. 1 μg RNA was used in a 20 μl cDNA synthesis reaction using oligo $(dT)_{18}$ primer and Moloney murine leukemia virus (MMLV) reverse transcriptase (Promega, Madison, WI, USA). cDNA mixture (2 μl) was used for PCR amplification. As a control, human β-actin cDNA was amplified to determine the integrity of the RNA and the efficiency of the cDNA synthesis. The primers were 5′-ACAAAATG-TTGCGTTCTCAGTCCA-3′ (sense) and 5′-CGTTTTGCCTTATCCATTCTCC-3′

(anti-sense) for Bfl1; 5′-TTGCCACAAATGGTGTGCTCTA-3′ (sense) and 5′-TCCTGGTGCCATGATTTACTGT-3′ for HCCS1; 5′-GATCAGCAAGCAGGAGTATGAC-3′ (sense) and 5′-ATGGCAAGGGACTTCCTGTAAC-3′ (antisense) for β-actin. These primers amplified the 302, 320 and 352 bp PCR products of Bfl1, HCCS1 and β-actin, respectively.

Gene transfection and analysis of cell death

Apoptotic cell death was monitored after transfection of expression plasmids into HEK293, HeLa, MCF-7 or BMK D3 cells. 2×10^5 cells were cultured in 35-mm wells for 24 hours in Dulbecco's modified Eagle's medium (DMEM) supplemented with 10% fetal bovine serum. Cells were transfected using the Lipofectamine 2000 reagent (Invitrogen), with 1 μg of the indicated expression plasmids and further cultured in the absence or presence of 50 μM of pan-caspase inhibitor, Q-VD-OPH (OPH, Enzyme Systems Products). For morphological assessment of apoptotic cell death, cells were plated onto LabTek II chamber slides (Nalgen Nunc International) at densities of 5×10^4 cells per well. 24 hours after transfection, cells were washed with phosphate- buffered saline (PBS) prior to fixation with 4% formaldehyde. Subsequently, cells were stained with a Vectasheild mounting solution (Vector Laboratories) containing 1 μg/ml of DAPI and visualized under an Axiovert 100 inverted epifluorescence microscope (Carl Zeiss). Nuclei with rippled contours and chromatin condensation were considered to represent the apoptotic cell death. Cell death was also measured by propidium iodide (PI) exclusion. After transfection with GFP fusion plasmids, a total of 1 μg/ml PI (Molecular Probes) was added to the cell culture medium. Cells were observed and photographed with a fluorescence microscope at three different fields containing approximately 200 GFP-positive cells. GFP and PI double-positive cells were counted as dead cells. Quantitative analysis of cell viability was determined by β-galactosidase reporter assay according to the procedures as described (Chittenden et al., 1995; Wood and Newcomb, 2000). Briefly, cells were co-transfected with 1 μg of tested plasmid plus 0.1 μg of pCMVβ (Sigma) plasmid expressing β-galactosidase. At 24 hours following transfection, cells were harvested and β-galactosidase activity was measured using β-Galactosidase Enzyme Assay System (Promega). In every experiment, each construct was tested in triplicate, and experiments were repeated at least three times. Cell viability is shown as the relative β-galactosidase activity to the control plasmid.

DNA fragmentation assay and flow cytometry

To analyze DNA fragmentation by agarose gel electrophoresis, cellular DNA was prepared as described (Essmann et al., 2003). 24 hours after transfection, cells in 35 mm wells were lysed in 0.2 ml lysis buffer (20 mM Tris-HCl, 0.5 mM EDTA, pH 8.0) containing 0.25% NP-40 and 50 μg RNase A at 37°C for 30 minutes. Each cell lysate was treated with 0.2 mg proteinase K for another 30 minutes at 37°C and centrifuged at 10,000 ***g*** for 10 minutes at 25°C. Supernatant containing fragmented DNA was analyzed on 2% agarose gel. DNA fragmentation was also determined by flow cytometry after DNA staining with PI. 24 hours after transfection, cells were washed twice with cold PBS and subsequently resuspended in PBS containing 50 μg/ml PI and 20 μg/ml RNaseA. Cells were incubated at room temperature for ~30 minutes prior to analysis and were protected from light. DNA contents were analyzed using Coulter Cytomics FC500 Flow Cytometer (Coulter Electronics).

Assessment of mitochondrial membrane potential and confocal microscopy

Mitochondrial membrane potential was measured following the protocol of Pratt and Niu (Pratt and Niu, 2003). Transiently transfected HeLa cells were incubated for 2 hours in medium containing 50 nM MitoTracker Red (CM-H_2 TMRos) (Molecular Probes), which develops fluorescence in cells with an intact mitochondrial membrane potential. Living cells were observed and photographed on a fluorescence microscope. MitoTracker-positive cells were counted from at least 200 GFP-positive cells. To observe intracellular localization of GFP fusion proteins, fixed HeLa cells were used for confocal microscopy. HeLa cells were transfected as described above on LabTek II chamber slides and cultured in the presence of 50 μM OPH. 18 hours after transfection, cells were stained with 50 nM MitoTracker Red (CM-H_2 TMRos) and washed with PBS followed by fixation with 4% formaldehyde. Cells finally were washed, mounted and analyzed with a confocal microscope Zeiss LSM 510 (Carl Zeiss Microscopy, Jena, Germany) equipped with a 63× objective. Image acquisition was performed at room temperature.

Western blotting

For western blotting, monoclonal anti-GFP antibody and anti-goat horseradish peroxidase (HRP) antibody were purchased from Santa Cruz Biotechnology. Anti-β-actin antibody was purchased from Sigma. The monoclonal anti-Flag 9E10.2 antibody was purchased from Invitrogen. The anti-mouse HRP antibody was purchased from Amersham Pharmacia. Monoclonal anti-cytochrome *c* 7H8.2C12 antibody, monoclonal anti-Bcl-xL 2H12 antibody, monoclonal anti-Bax 6A7 antibody, Polyclonal anti-Bak antibody were purchased from BD Biosciences, Sigma, Zymed Laboratory and from Upstate Biotechnology, respectively. For immunoblot analysis, 20 μg of protein was subjected to SDS-PAGE and transferred onto a PVDF membrane, which was blocked with 5% skimmed milk, probed with primary antibodies and visualized using an ECL chemiluminescence kit (Amersham Pharmacia).

Peptide synthesis and lipid bilayer experiment

The 29-mer ATAP peptide (KFEPKSGWMTFLEVTGKICEMLSLLKQYC) corresponding to the C-terminus of Bfl1 and its mutant mHR7 (KFEPKSGWMTFLQVTG-LICQMLSLLKQYC) were synthesized by Abgent (San Diego, CA) with 99% purity as measured by HPLC and mass spectrometry. The peptides were dissolved in DMSO to make a 10 mM stock. Phospholipids were purchased from Avanti Polar Lipids (Birmingham, AL). Electrophysiological analysis was performed as described (Lam et al., 1998; Ma et al., 1988). Lipid bilayer membranes were formed across an aperture of 200 μm diameter with a 1:1 mixture of bovine brain phosphatidylethanolamine and bovine brain phosphatidylserine dissolved in n-decane at a concentration of 50 mg/ml. The recording solutions contained: *cis*, 200 mM KCl and 10 mM HEPES-Tris (pH 7.4); *trans*, 50 mM NaCl, 10 mM HEPES-Tris (pH 7.4). 1 μl of 10 mM peptides dissolved in DMSO were added into 900 μl of *cis* solution and fused into the bilayer. Voltage manipulation and currents were measured using an Axopatch 200A amplifier (Axon Instruments, Foster City, CA). Data analyses were preformed with pClamp and TIPS software.

Assay for cytochrome c release from mitochondria

Mitochondria-free cytosol was prepared as previously described (Ko et al., 2003a). Briefly, 24 hours after transfection, HEK293 cells were collected by scraping, washed twice with ice-cold PBS, suspended in 100 μl extraction buffer (50 mM PIPES-KOH, pH 7.4, 200 mM mannitol, 70 mM sucrose, 50 mM KCl, 5 mM EGTA, 2 mM $MgCl_2$, 1 mM dithiothreitol and protease inhibitors), and incubated on ice for 30 minutes. Cells were lysed by Dounce homogenization and homogenates were centrifuged at 100,000 ***g*** for 15 minutes at 4°C. Supernatants were harvested and 20 μg of protein was analyzed by western blotting using monoclonal anti-cytochrome c antibody. For in vitro analysis of cytochrome c release, heavy membranes enriched in mitochondria were isolated from BMK-D3 cells using a mitochondria fractionation kit (Active Motif) according to the instructions of the manufacturer. Isolated mitochondria were diluted to a concentration of 1 mg/ml in the extraction buffer and incubated with synthetic ATAP or mHR7 peptides (100 μM) or DMSO as control for 1 hour at 37°C. The reactions were then centrifuged at 13,000 ***g*** for 10 minutes and the resulting pellets and supernatants were analyzed by SDS-PAGE.

This work was supported by NIH grants to J.M. (RO1-CA95739, RO1-AG15556, RO1-HL69000 and RO1-AG28614) and partly by the Korea Science & Engineering Foundation (KOSEF) through the Tumor Immunity MRC to C.W.K. We thank Eileen White for the generous donation of BMK D3 cells, and Robert E. Campbell for providing the pRSETB-mRFP vector.

References

Borgese, N., Colombo, S. and Pedrazzini, E. (2003). The tale of tail-anchored proteins: coming from the cytosol and looking for a membrane. *J. Cell Biol.* **161**, 1013-1019.

Campbell, R. E., Tour, O., Palmer, A. E., Steinbach, P. A., Baird, G. S., Zacharias, D. A. and Tsien, R. Y. (2002). A monomeric red fluorescent protein. *Proc. Natl. Acad. Sci. USA* **99**, 7877-7882.

Chen, Y., Xu, X., Hong, S., Chen, J., Liu, N., Underhill, C. B., Creswell, K. and Zhang, L. (2001). RGD-Tachyplesin inhibits tumor growth. *Cancer Res.* **61**, 2434-2438.

Cheng, E. H., Kirsch, D. G., Clem, R. J., Ravi, R., Kastan, M. B., Bedi, A., Ueno, K. and Hardwick, J. M. (1997). Conversion of Bcl-2 to a Bax-like death effector by caspases. *Science* **278**, 1966-1968.

Cheng, Q., Lee, H. H., Li, Y., Parks, T. P. and Cheng, G. (2000). Upregulation of Bcl-x and Bfl-1 as a potential mechanism of chemoresistance, which can be overcome by NF-kappaB inhibition. *Oncogene* **19**, 4936-4940.

Chittenden, T., Flemington, C., Houghton, A. B., Ebb, R. G., Gallo, G. J., Elangovan, B., Chinnadurai, G. and Lutz, R. J. (1995). A conserved domain in Bak, distinct from BH1 and BH2, mediates cell death and protein binding functions. *EMBO J.* **14**, 5589-5596.

Clem, R. J., Cheng, E. H., Karp, C. L., Kirsch, D. G., Ueno, K., Takahashi, A., Kastan, M. B., Griffin, D. E., Earnshaw, W. C., Veliuona, M. A. et al. (1998). Modulation of cell death by Bcl-XL through caspase interaction. *Proc. Natl. Acad. Sci. USA* **95**, 554-559.

Cory, S. and Adams, J. M. (2002). The Bcl2 family: regulators of the cellular life-or-death switch. *Nat. Rev. Cancer* **2**, 647-656.

Cuff, J. A., Clamp, M. E., Siddiqui, A. S., Finlay, M. and Barton, G. J. (1998). JPred: a consensus secondary structure prediction server. *Bioinformatics* **14**, 892-893.

Degenhardt, K., Sundararajan, R., Lindsten, T., Thompson, C. and White, E. (2002). Bax and Bak independently promote cytochrome *c* release from mitochondria. *J. Biol. Chem.* **277**, 14127-14134.

Duriez, P. J., Wong, F., Dorovini-Zis, K., Shahidi, R. and Karsan, A. (2000). A1

functions at the mitochondria to delay endothelial apoptosis in response to tumor necrosis factor. *J. Biol. Chem.* **275**, 18099-18107.

Ellerby, H. M., Arap, W., Ellerby, L. M., Kain, R., Andrusiak, R., Rio, G. D., Krajewski, S., Lombardo, C. R., Rao, R., Ruoslahti, E. et al. (1999). Anti-cancer activity of targeted pro-apoptotic peptides. *Nat. Med.* **5**, 1032-1038.

Emanuelsson, O., Nielsen, H., Brunak, S. and von Heijne, G. (2000). Predicting subcellular localization of proteins based on their N-terminal amino acid sequence. *J. Mol. Biol.* **300**, 1005-1016.

Essmann, F., Bantel, H., Totzke, G., Engels, I. H., Sinha, B., Schulze-Osthoff, K. and Janicke, R. U. (2003). Staphylococcus aureus alpha-toxin-induced cell death: predominant necrosis despite apoptotic caspase activation. *Cell Death Differ.* **10**, 1260-1272.

Geourjon, C. and Deleage, G. (1995). SOPMA: significant improvements in protein secondary structure prediction by consensus prediction from multiple alignments. *Comput. Appl. Biosci.* **11**, 681-684.

Gross, A., McDonnell, J. M. and Korsmeyer, S. J. (1999). BCL-2 family members and the mitochondria in apoptosis. *Genes Dev.* **13**, 1899-1911.

Holmgreen, S. P., Huang, D. C., Adams, J. M. and Cory, S. (1999). Survival activity of Bcl-2 homologs Bcl-w and A1 only partially correlates with their ability to bind pro-apoptotic family members. *Cell Death Differ.* **6**, 525-532.

Janicke, R. U., Sprengart, M. L., Wati, M. R. and Porter, A. G. (1998). Caspase-3 is required for DNA fragmentation and morphological changes associated with apoptosis. *J. Biol. Chem.* **273**, 9357-9360.

Johnston, A. J., Hoogenraad, J., Dougan, D. A., Truscott, K. N., Yano, M., Mori, M., Hoogenraad, N. J. and Ryan, M. T. (2002). Insertion and assembly of human tom7 into the preprotein translocase complex of the outer mitochondrial membrane. *J. Biol. Chem.* **277**, 42197-42204.

Kaufmann, T., Schlipf, S., Sanz, J., Neubert, K., Stein, R. and Borner, C. (2003). Characterization of the signal that directs Bcl-x(L), but not Bcl-2, to the mitochondrial outer membrane. *J. Cell Biol.* **160**, 53-64.

Kim, T. E., Kim, Y. W., Hwang, S. Y., Shin, S. M., Shin, J. W., Lee, Y. H., Shin, S. Y., Han, K. T., Lee, J. M., Namkoong, S. E. et al. (2002). Candidate tumor suppressor, HCCS-1, is downregulated in human cancers and induces apoptosis in cervical cancer. *Int. J. Cancer* **97**, 780-786.

Ko, J. K. and Ma, J. (2005). A rapid and efficient PCR-based mutagenesis method applicable to cell physiology study. *Am. J. Physiol. Cell Physiol.* **288**, C1273-C1278.

Ko, J. K., Choi, K. H., Kim, H. J., Choi, H. Y., Yeo, D. J., Park, S. O., Yang, W. S., Kim, Y. N. and Kim, C. W. (2003a). Conversion of Bfl-1, an anti-apoptotic Bcl-2 family protein, to a potent pro-apoptotic protein by fusion with green fluorescent protein (GFP). *FEBS Lett.* **551**, 29-36.

Ko, J. K., Lee, M. J., Cho, S. H., Cho, J. A., Lee, B. Y., Koh, J. S., Lee, S. S., Shim, Y. H. and Kim, C. W. (2003b). Bfl-1S, a novel alternative splice variant of Bfl-1, localizes in the nucleus via its C-terminus and prevents cell death. *Oncogene* **22**, 2457-2465.

Kucharczak, J. F., Simmons, M. J., Duckett, C. S. and Gelinas, C. (2005). Constitutive proteasome-mediated turnover of Bfl-1/A1 and its processing in response to TNF receptor activation in FL5.12 pro-B cells convert it into a prodeath factor. *Cell Death Differ.* **12**, 1225-1239.

Kushnareva, Y. E., Polster, B. M., Sokolove, P. M., Kinnally, K. W. and Fiskum, G. (2001). Mitochondrial precursor signal peptide induces a unique permeability transition and release of cytochrome *c* from liver and brain mitochondria. *Arch. Biochem. Biophys.* **386**, 251-260.

Lam, M., Bhat, M. B., Nunez, G., Ma, J. and Distelhorst, C. W. (1998). Regulation of Bcl-xl channel activity by calcium. *J. Biol. Chem.* **273**, 17307-17310.

Letai, A., Bassik, M. C., Walensky, L. D., Sorcinelli, M. D., Weiler, S. and Korsmeyer, S. J. (2002). Distinct BH3 domains either sensitize or activate mitochondrial apoptosis, serving as prototype cancer therapeutics. *Cancer Cell* **2**, 183-192.

Ma, J., Fill, M., Knudson, C. M., Campbell, K. P. and Coronado, R. (1988). Ryanodine receptor of skeletal muscle is a gap junction-type channel. *Science* **242**, 99-102.

Mai, J. C., Mi, Z., Kim, S. H., Ng, B. and Robbins, P. D. (2001). A proapoptotic peptide for the treatment of solid tumors. *Cancer Res.* **61**, 7709-7712.

Motz, C., Martin, H., Krimmer, T. and Rassow, J. (2002). Bcl-2 and porin follow different pathways of TOM-dependent insertion into the mitochondrial outer membrane. *J. Mol. Biol.* **323**, 729-738.

Muro, C., Grigoriev, S. M., Pietkiewicz, D., Kinnally, K. W. and Campo, M. L. (2003). Comparison of the TIM and TOM channel activities of the mitochondrial protein import complexes. *Biophys. J.* **84**, 2981-2989.

Nielsen, H., Engelbrecht, J., Brunak, S. and von Heijne, G. (1997). Identification of prokaryotic and eukaryotic signal peptides and prediction of their cleavage sites. *Protein Eng.* **10**, 1-6.

Pan, Z., Damron, D., Nieminen, A. L., Bhat, M. B. and Ma, J. (2000). Depletion of intracellular Ca2+ by caffeine and ryanodine induces apoptosis of chinese hamster ovary cells transfected with ryanodine receptor. *J. Biol. Chem.* ***275***, 19978-19984.

Pan, Z., Bhat, M. B., Nieminen, A. L. and Ma, J. (2001). Synergistic movements of Ca(2+) and Bax in cells undergoing apoptosis. *J. Biol. Chem.* **276**, 32257-32263.

Petit, P. X., Lecoeur, H., Zorn, E., Dauguet, C., Mignotte, B. and Gougeon, M. L. (1995). Alterations in mitochondrial structure and function are early events of dexamethasone-induced thymocyte apoptosis. *J. Cell Biol.* **130**, 157-167.

Pratt, M. A. and Niu, M. Y. (2003). Bcl-2 controls caspase activation following a p53-dependent cyclin D1-induced death signal. *J. Biol. Chem.* **278**, 14219-14229.

Schimmer, A. D., Hedley, D. W., Chow, S., Pham, N. A., Chakrabartty, A., Bouchard, D., Mak, T. W., Trus, M. R. and Minden, M. D. (2001). The BH3 domain of BAD fused to the Antennapedia peptide induces apoptosis via its alpha helical structure and independent of Bcl-2. *Cell Death Differ.* **8**, 725-733.

Schleiff, E., Shore, G. C. and Goping, I. S. (1997). Human mitochondrial import receptor, Tom20p. Use of glutathione to reveal specific interactions between Tom20-glutathione S-transferase and mitochondrial precursor proteins. *FEBS Lett.* **404**, 314-318.

Shai, Y. and Oren, Z. (2001). From "carpet" mechanism to de-novo designed diastereomeric cell-selective antimicrobial peptides. *Peptides* **22**, 1629-1641.

Smaili, S. S., Hsu, Y. T., Sanders, K. M., Russell, J. T. and Youle, R. J. (2001). Bax translocation to mitochondria subsequent to a rapid loss of mitochondrial membrane potential. *Cell Death Differ.* **8**, 909-920.

Walensky, L. D., Kung, A. L., Escher, I., Malia, T. J., Barbuto, S., Wright, R. D., Wagner, G., Verdine, G. L. and Korsmeyer, S. J. (2004). Activation of apoptosis in vivo by a hydrocarbon-stapled BH3 helix. *Science* **305**, 1466-1470.

Wang, C. Y., Guttridge, D. C., Mayo, M. W. and Baldwin, A. S., Jr (1999). NF-kappaB induces expression of the Bcl-2 homologue A1/Bfl-1 to preferentially suppress chemotherapy-induced apoptosis. *Mol. Cell. Biol.* **19**, 5923-5929.

Werner, A. B., de Vries, E., Tait, S. W., Bontjer, I. and Borst, J. (2002). Bcl-2 family member Bfl-1/A1 sequesters truncated bid to inhibit is collaboration with pro-apoptotic Bak or Bax. *J. Biol. Chem.* **277**, 22781-22788.

Wood, D. E. and Newcomb, E. W. (2000). Cleavage of Bax enhances its cell death function. *Exp. Cell Res.* **256**, 375-382.

Yang, W. S., Ko, J. K., Park, S. O., Choi, H. Y., Kim, Y. N. and Kim, C. W. (2005). C-terminal region of Bfl-1 induces cell death that accompanies caspase activation when fused with GFP. *J. Cell. Biochem.* **94**, 1234-1247.

Zamzami, N., Marchetti, P., Castedo, M., Zanin, C., Vayssiere, J. L., Petit, P. X. and Kroemer, G. (1995). Reduction in mitochondrial potential constitutes an early irreversible step of programmed lymphocyte death in vivo. *J. Exp. Med.* **181**, 1661-1672.

Zhang, H., Cowan-Jacob, S. W., Simonen, M., Greenhalf, W., Heim, J. and Meyhack, B. (2000). Structural basis of BFL-1 for its interaction with BAX and its anti-apoptotic action in mammalian and yeast cells. *J. Biol. Chem.* **275**, 11092-11099.

Zong, W. X., Edelstein, L. C., Chen, C., Bash, J. and Gelinas, C. (1999). The prosurvival Bcl-2 homolog Bfl-1/A1 is a direct transcriptional target of NF-kappaB that blocks TNFalpha-induced apoptosis. *Genes Dev.* **13**, 382-387.

Supplementary tables

Table S1. Primer pairs for construction of expression vectors

Primer name	Primer sequence	Construct
ATAP-F	5'-AA**CTCGAG**CTAAGTTTGAACCTAAATCTGGC	pGFP-ATAP
ATAP-R	5'-TT**GAATTC**AACAGTATTGCTTCAGGAGAGAT	
TAxL-F	5'-AA**CTCGAG**CTGAGAGCCGAAAGGGCCAG	pGFP-TAxL
TAxL-R	5'-TT**GAATTC**ATTTCCGACTGAAGAGTGAGCC	
HCCS-F1	5'-AA**CTCGAG**GCCACCATGAGAGTTTCATTCTGTCGCCC	pHCCS-1-GFP
HCCS-R1	5'-AA**GAATTC**GAAAGTAGAAGTATGTGTTGGC	
HCCS-F2	5'-AA**CTCGAG**GCCACCATGACTGCAACCTCTGTCTCC	pHCCS-1 (ΔMTS)-GFP
HCCS-R2	5'-AA**GAATTC**GAAAGTAGAAGTATGTGTTGGC	
HCCS-F3	5'-AA**CTCGAG**GCCACCATGAGAGTTTCATTCTGTCGCCC	pMTS-GFP
HCCS-R3	5'-AA**GAATTC**GGAGCCGAGATCGCGCCATTG	
HCCS-F4	5'-AA**TCCGGA**GAAAATGGCTTTGTAAAGAAGCTTGA	pGFP-HCCS-1 (ΔMTS)
HCCS-R4	5'-AA**GAATTC**AAAAGTAGAAGTATGTGTTGGCAATCG	
HCCS-F5	5'-AA**TCCGGA**AAGAAGCTTGAGCCTAAATCTGGC	pGFP-ATAP (HCCS-1)
HCCS-R5	5'-AA**GAATTC**AACAATATGGAGTGTCCTTTCTGGT	
mRFP-mito-F	5'-AA**GCTAGC**GCCACCATGGATTATAAGGACGATGACGATAAG	pmRFP-mito
mRFP-mito-R	5'-AA**TCCGGA**ATAGGCGCCGGTGGAGTGGCG	

Table S2. Primers pairs for construction of mFR mutants of ATAP

Primer name	Primer sequence	Construct
K1L-F	5'-AA**CTCGAG**CTCTGTTTGAACCTAAATCTGGCTGG	mFR1
ATAP-R	5'-TT**GAATTC**AACAGTATTGCTTCAGGAGAGAT	
K5L-F	5'-AA **CTCGAG**CTAAGTTTGAACCTCTATCTGGCTGGATGACTTTT	mFR2
ATAP-R	5'-TT**GAATTC**AACAGTATTGCTTCAGGAGAGAT	
ATAP-F	5'-AA**CTCGAG**CTAAGTTTGAACCTAAATCTGGC	mFR3
K26L-R	5'-TT**GAATTC**AACAGTATTGCAGCAGGAG AGATAGCATTTCAC	
K1,5L-F	5'-AA**CTCGAG**CTCTGTTTGAACCTCTATCTGGCTGGATGACTTTT	mFR4
ATAP-R	5'-TT**GAATTC**AACAGTATTGCTTCAGGAGAGAT	
K1L-F	5'-AA**CTCGAG**CTCTGTTTGAACCTAAATCTGGCTGG	mFR5
K26L-R	5'-TT**GAATTC**AACAGTATTGCAGCAGGAG AGATAGCATTTCAC	
K5L-F	5'-AA **CTCGAG**CTAAGTTTGAACCTCTATCTGGCTGGATGACTTTT	mFR6
K26L-R	5'-TT**GAATTC**AACAGTATTGCAGCAGGAG AGATAGCATTTCAC	
K1,5L-F	5'-AA**CTCGAG**CTCTGTTTGAACCTCTATCTGGCTGGATGACTTTT	mFR7
K26L-R	5'-TT**GAATTC**AACAGTATTGCAGCAGGAG AGATAGCATTTCAC	

Table S3. Primer pairs for construction of mHR mutants of ATAP

Primer name	Primer sequence	Construct
E13Q-F	5′-AA**CTCGAG**CTAAGTTTGAACCTAAATCTGGCTGGATGACTTTTCTACAA***GTTACAGGAAAGATCTGT***	mHR1
sTA-R	5′-TT**GAATTC**AACAGTATTGCTTCAGGAGAGATAGCATTTC***ACAGATCTTTCCTGTAACTT***	
sTA-F	5′-AA**CTCGAG**CTAAGTTTGAACCTAAATCTGGCTGGATGACTTTTCTAGAA***GTTACAGGAAAGATCTGT***	mHR2
E20Q-R	5′-TT**GAATTC**AACAGTATTGCTTCAGGAGAGATAGCATTTG***ACAGATCTTTCCTGTAACTT***	
E13Q-F	5′-AA**CTCGAG**CTAAGTTTGAACCTAAATCTGGCTGGATGACTTTTCTACAA***GTTACAGGAAAGATCTGT***	mHR3
E20Q-R	5′-TT**GAATTC**AACAGTATTGCTTCAGGAGAGATAGCATTTG***ACAGATCTTTCCTGTAACTT***	
E13L-F	5′-AA**CTCGAG**CTAAGTTTGAACCTAAATCTGGCTGGATGACTTTTCTACTA***GTTACAGGAAAGATCTGT***	mHR4
E20L-R	5′-TT**GAATTC**AACAGTATTGCTTCAGGAGAGATAGCATTAG***ACAGATCTTTCCTGTAACTT***	
E13K-F	5′-AA**CTCGAG**CTAAGTTTGAACCTAAATCTGGCTGGATGACTTTTCTAAAG***GTTACAGGAAAGATCTGT***	mHR5
E20K-R	5′-TT**GAATTC**AACAGTATTGCTTCAGGAGAGATAGCATCTT***ACAGATCTTTCCTGTAACTT***	
K17L-F	5′-AA**CTCGAG**CTAAGTTTGAACCTAAATCTGGCTGGATGACTTTTCTAGAA***GTTACAGGACTAATCTGT***	mHR6
K17L-R	5′-TT**GAATTC**AACAGTATTGCTTCAGGAGAGATAGCATTTC***ACAGATTAGTCCTGTAACTT***	
KE2L-F	5′-AA**CTCGAG**CTAAGTTTGAACCTAAATCTGGCTGGATGACTTTTCTACAA***GTTACAGGACTAATCTGT***	mHR7
KE2L-R	5′-TT**GAATTC**AACAGTATTGCTTCAGGAGAGATAGCATTTG***ACAGATTAGTCCTGTAACTT***	